Substituent Effects and Correlations of Electrochemical Behaviors with Molecular Orbital Calculation of Thioxantone Derivatives I

Kyeong-Do Kwak, Moo Lyong Seo, Kwang Soo Ha, and U-Hyon Paek*

Department of Chemistry, Gyeongsang National University, Chinju 660-701, Korea
Received September 18, 1997

This paper presents the electrochemistry and molecular orbital (MO) picture of a series of conformationally-restricted thioxantone derivatives. A series of C_2-substituted thioxanthones were examined to probe the electronic influence of the substituent on the electrooxidation and electroreduction sites (*i.e.*, on the electron densities at the 10- and 9-positions), respectively. In the presence of "electrophoric" groups such as C=O and S, characteristic electrochemical reduction and oxidation responses are observed. The electrochemical reaction was diffusion-controlled, because the $i_p/\upsilon^{1/2}$ ratio was constant for the anodic and cathodic wave of thioxantone derivatives. These substituent effects are presented in terms of correlations of oxidation (or reduction) potentials with the highest occupied molecular orbital (HOMO), or lowest unoccupied molecular orbital (LUMO) energies, respectively. There is good correlation between energies of the HOMO *vs.* $E_{pa}^{(+)}$ and energies of the LUMO *vs.* $E_{pc}^{(-)}$. Frontier Molecular Orbital (FMO) is changed by the functional group of thioxanthones. FMO energy level was offered us the information about the electron transfer direction, and the coefficient of FMO was offered the information about the electron transfer position. Sulfur atom has an important effect on oxidation potential, $E_{pa}^{(+)}$ and the carbonyl carbon has an important effect on reduction potential, $E_{pc}^{(-)}$. Therefore we were appreciated that the contribution of sulfur atom for the $E_{pa}^{(+)}$ and HOMO energies is larger than the contribution of carbonyl group for the $E_{pc}^{(-)}$ and LUMO energies.

Introduction

Thioxantone derivatives have been shown to possess two useful properties such as medicinal[1] and photoinitiation activity.[2,3] They can exist in a multitude of conformations each having potential for its own chemical and spectroscopic properties. In order to understand the effect of geometry upon relation and properties, many researchers have devoted considerable effort in the studies of the chemistry of derivatives of thioxantone.[4]

Thioxantone exhibits varying degrees of folding about the imaginary line containing C=O and S (the "meso" position). In folded structures, the non-bonding electrons on sulfur exist in two distinctly different environments. One of these (pseudo-axial, a') is parallel to the aryl π system and may be thought of as "truly" benzylic, while the other (pseudo-equatorial, e') is essentially orthogonal to the aryl π network and is only "formally" benzylic.

Because of the electron of pseudo-axial was in resonance with aryl π system, thioxantone has resonance structure[5] (Figure 1).

Also, because of the planarity of their central, ring bond unit of O^--C_9=C-C_1=C_2-C_3=C_4-C=S_{10} has been odd-alternant conjugation system. In these systems, coefficient of FMO has non zero charge at only star position (Figure 1). Substituentes of this position have affected electronic structure of FMO. Therefore, C_2-substituted thioxantone derivatives will be affected to reduction of carbonyl group of C_9 position and oxidation of S_{10} from resonance and induced effect.

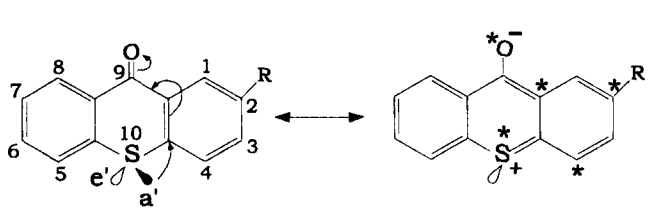

Figure 1. Resonance structures of thioxantone.

In order to understand these stereochemical properties, this paper has studied the correlation of electrochemical behavior and HOMO energies, or LUMO energies of thioxantone derivatives, respectively.

Experimental

Thioxanthone derivatives were prepared according to the literature method[6] and identified by IR, NMR spectroscopy and elemental ananlysis. ^{1}H NMR and ^{13}C NMR and IR spectra were obtained in the Fourier transform mode with Varian Unity Plus 300 and Hitachi 270-50, respectively. Also data of elements analysis were obtained with Perkin Elmer 240C.

Cyclic voltammetry (CV) was performed in "dry" acetonitrile. The solvent was obtained by distillation of HPLC-grade solvent (Aldrich Co.) over P_2O_5. Tetraethylammonium perchlorate (TEAP)[7] was used as supporting electrolyte (0.1 M). Three electrode cell geometry with feedback IR compensation was used in all cases; all measurements pertain to ambient temperature.

BAS CV 50W (U.S.A.) electrochemical system was used in conjunction with an IBM Instruments Inc. The working electrode was Pt with a nominal geometric area of 0.20 cm^2; the reference electrode was Ag/Agcl.

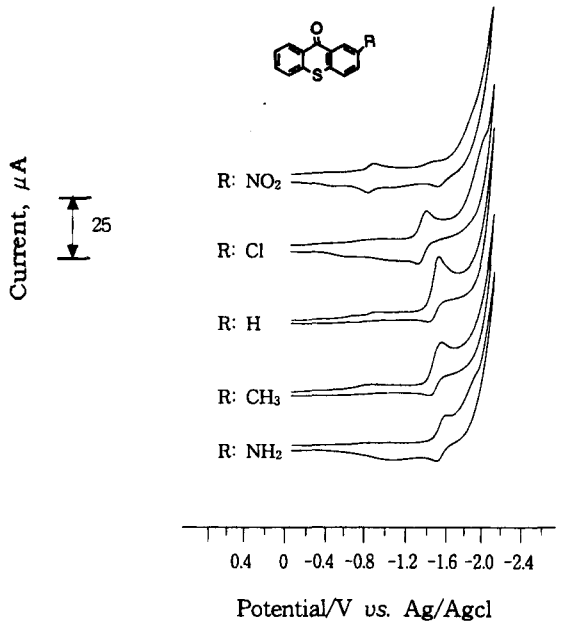

Figure 2. Cyclic voltammograms of 1 mM thioxanthone derivatives in 0.1 M TEAP-acetonitrile solution, scan rate: 100 mV/s.

Results and Discussion

Electrochemical behaviors of thioxantone derivatives. The electrochemical behaviors of thioxantone derivatives in acetonitrile were investigated by cyclic voltammetry (CV) at Pt electrode. The CV scans were performed in the usual manner, by first moving the potential in the positive direction and subsequently in the negative direction, starting from the rest potential. Typical cyclic voltammetry for reduction-processes of 1 mM thioxanthone derivatives in acetonitrile is shown in Figure 2.

As can be seen in Figure 2, the redox processes were nearly reversible. Also, a summary of the redox process observed for the thioxantone derivatives in acetonitrile is listed in Table 1. The superscript "(+)" and "(-)" (*e.g.*, $E_{pa}^{(+)}$, $E_{pc}^{(-)}$) denote oxidation and reduction branches respectively for given compounds.

Figure 3 shows the cyclic voltammograms of 1 mM 2-amino thioxanthone in acetonitrile solution at various scan rates. As can be seen in Figure 3, The electrochemical reaction was diffusion-controlled, because the $i_p/\upsilon^{1/2}$ ratio was constant for the anodic wave of 2-amino thioxanthone.

Correlation of electrochemical behaviors with MO calculations. Correlation of voltammetric peak potentials with Hückel MO parameters has been presented for a variety of compounds. If one electron transfer reaction was occurred, $E_{pa}^{(+)}$ and $E_{pc}^{(-)}$ should scale with the energies of the HOMO and the LUMO respectively.[8,9] Notwithstanding complications from electrochemical irreversibility (kinetic complications) and entropic/solvation contributions, correlations (*e.g.*, $E_{pa}^{(+)}$ *vs.* ionization potential) have been surprisingly good.[10]

Table 1. The values of $E_{pa}^{(+)}$, $E_{pc}^{(-)}$ (V *vs.* Ag/Agcl), E_{HOMO} and E_{LUMO} (eV) of thioxanthone derivatives

R	$E_{pa}^{(+)}$	$E_{pc}^{(-)}$	E_{HOMO}	E_{LUMO}
NH_2	1.145	−1.524	−0.278	0.067
CH_3	1.186	−1.483	−0.303	0.064
H	1.220	−1.464	−0.309	0.063
Cl	1.244	−1.326	−0.316	0.507
NO_2	1.325	−0.801	−0.333	0.032

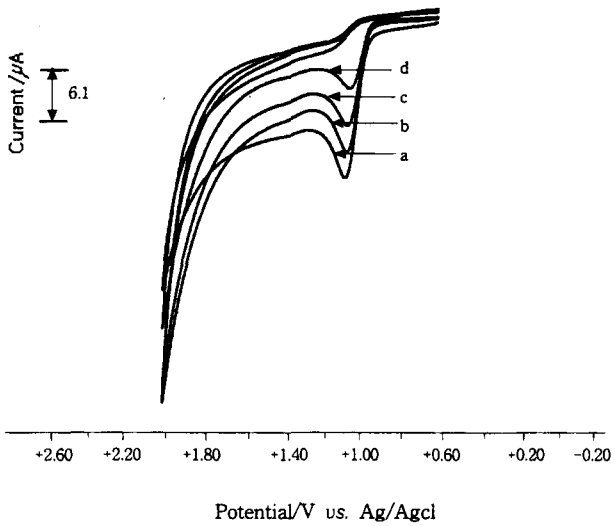

Figure 3. Cyclic voltammograms of 1 mM 2-amino thioxanthone containing 0.1 M TEAP in acetonitrile solution. scan rate: (a) 100, (b) 80, (c) 50, (d) 20 mV/s.

Thus the computation were performed with Hyperchem 5.0 program packages.[11] All the calculation of functional thioxanthones have been performed with the RHF/3-21G level.[12-14] The geometry of the functional thioxanthones were completely optimized by using Polak-Ribiere method.[15] Some electrochemical and quantum chemical values of functional thioxanthones are shown in Table 1. The typical correlations are presented in Figure 4.

One electron transfer reaction was occurred for thioxanthone derivatives.[5] Therefore as can be seen in Figure 4, there is a good correlation between energy of the HOMO *vs.* $E_{pa}^{(+)}$ and energy of the LUMO *vs.* $E_{pc}^{(-)}$. The following expression describe the variation of $E_{pa}^{(+)}$ and $E_{pc}^{(-)}$ respectively with the HOMO and LUMO energies for the various compounds in this series.

$$E_{pa}^{(+)} = -3.21\ E_{HOMO} - 0.23$$

$$E_{pc}^{(-)} = -20.96\ E_{LUMO} - 0.15$$

The relationship between LUMO energy and $E_{pc}^{(-)}$ show good linear shape within 0.96(=R^2, This is the coefficient of simple determent). The value of R^2 for the HOMO *vs.* $E_{pa}^{(+)}$ is 0.91.

The FMO (HOMO+LUMO) energy levels give us the information about the electron transfer direction, and the coefficients of FMO give us the information about the electron transfer position.

FMO energy level is changed by the functional group of thioxanthones. As can be seen in Table 1, electron donating group (EDG) push up FMO level and electron withdrawing group (EWG) push down FMO level. The higher HOMO

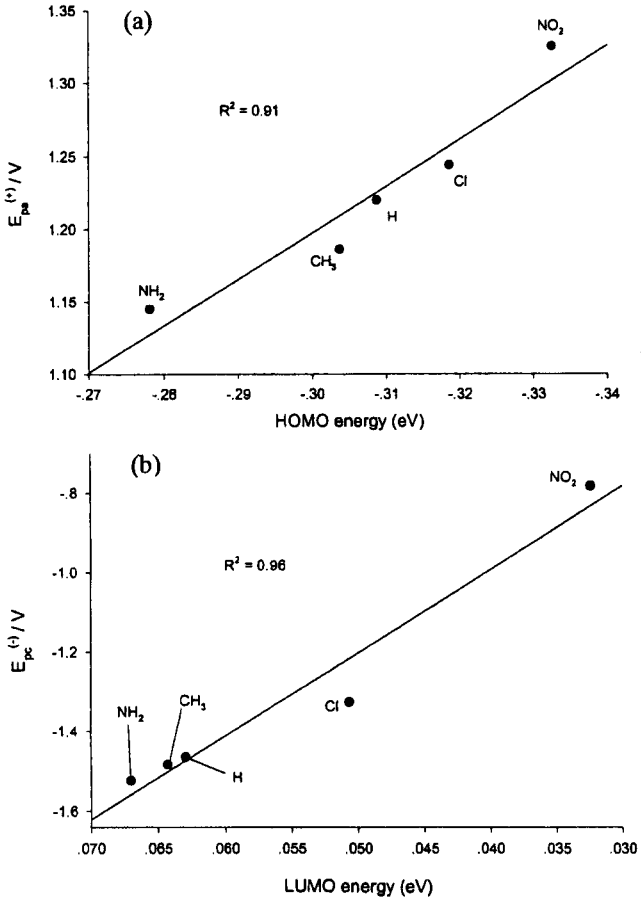

Figure 4. Correlation of $E_{pa}^{(+)}$ with HOMO energies (a) and $E_{pc}^{(-)}$ with LUMO energies (b) for thioxantone derivatives. The MO energies were computed by the RHF/3-21G level.

energy level goes up by EDG, the easier HOMO electron leave functional thioxanthones. This effect causes the values of $E_{pa}^{(+)}$ to decrease. Also, the lower HOMO energy level goes down by EWG, the more hard HOMO electron leave functional thioxanthones. This effect causes the values of $E_{pa}^{(+)}$ to increase.

The lower LUMO energy level goes down by EWG, the easier it accepts electrons. This effect causes the values of $E_{pc}^{(-)}$ to decrease. The higher LUMO energy level goes up by EDG, the more hard it accepts electrons. This effect causes the values of $E_{pc}^{(-)}$ to increase.

The HOMO orbital coefficient for the sulfur atom and the LUMO orbital coefficient for the carbonyl atom have larger value than it of other atoms. These experimental and quantum chemical facts lead to conclude that the linked plane of sulfur-carbon-oxygen is important in this reaction. We showed the methylthioxanthone's SCO plane in the Figure 5.

The carbonyl carbon's contribution for the LUMO orbital is less important than sulfur's contribution for the HOMO orbital. The LUMO orbital coefficient is more widely distributive than HOMO's.

In these results, FMO energy level is changed by the functional group of thioxanthones. If FMO energy level is changed by EDG or EWG, FMO electron's moving cause the $E_{pa}^{(+)}$ or $E_{pc}^{(-)}$ change.

Sulfur atom has an important effect on oxidation potential,

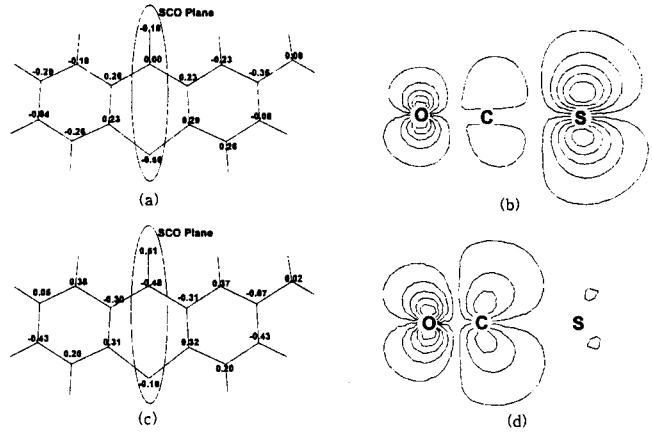

Figure 5. The linked plane of sulfur-carbon-oxygen (SCO). (a) HOMO orbital coefficients of the methylothioxanthone. (b) Contour line of HOMO orbital for the methylthioxanthone SCO plane (c) LUMO orbital coefficients of methylthioxanthone (d) Contour line of LUMO orbital for the methylthioxanthone SCO plane.

$E_{pa}^{(+)}$ and the carbonyl carbon has an important effect on reduction potential, $E_{pc}^{(-)}$. However we were appreciated that the contribution of sulfur atom for the $E_{pa}^{(+)}$ and HOMO energies is larger than the contribution of carbon for the $E_{pc}^{(-)}$ and LUMO energies.

Acknowledgment. We would like thank Professor Yong Jin Yoon for supplying the series materials of thioxanthone.

References

1. Honek, J. F.; Mancinl, M. L.; Belleau, B. *Synth. Commun.* **1983**, *13*, 977.
2. Monroe, B. M.; Weed, G. C. *Chem. Rev.* **1993**, *93*, 435.
3. Angiolini, L.; Carett, D.; Carlini, C.; Fouassier, J. P.; Morletsavary, F. O. *Polymer* **1995**, *36*, 21.
4. Caira, M. R.; Watson, W. H.; Ternay, A. L.; McKellar, R. *Acta Crystallor* **1984**, *C40*, 842.
5. Tasi, E. W.; Throckmorton, L.; McKellar, R.; Baar, M.; Kluba, M.; Marynick, D. S.; Rajeshwar, K.; Ternay, A. L. *J. Electroanal. Chem.* **1986**, *210*, 45.
6. Moon, J. G. *in studies on Thioxanthone Derivation*; Ph. D thesis, 1977. Geongsang National University, Korea.
7. Kolthoff, I. M.; Coetzee, J. F. *J. Am. Chem. Soc.* **1957**, *79*, 1852.
8. Bowen, H. J. M.; Donohue, J.; Jenkin, D. G.; Kenna, O.; Wheatley, P. J.; Shiffen, D. H. *The Chemical Society*; London: 1958, No. 11.
9. (a) Lynton, H.; Cox, E. G. *J. Chem. Soc.* **1956**, 4886. (b) Schraffin, R. M.; Trotter, J. *J. Chem. Soc. A*, **1970**, 1561. (c) Shirley, S. C. C.; Yang, H. T. *Acta Crystallogr* **1977**, *B33*, 2991.
10. (a) Miller, L. L.; Nordblom, G. D.; Mayeda, E. A. *J. Org. Chem.* **1972**, *37*, 916. (b) Gassman, P. G.; Mullins, M. J.; Richtsmeir, S.; Dixon, D. A. *J. Am. Chem. Soc.* **1979**, *101*, 5793.
11. Hypercube, Hyperchem, Autodesk, Inc., 1996.
12. Binkley, J. S.; Pople, J. A.; Hehre, W. J. *J. Am. Chem. Soc.* **1980**, *102*, 939.

13. Gordon, M. S.; Binkley, J. S.; Pople, J. A.; Pietro, W. J.; Hehre, W. J. *J. Am. Chem. Soc.* **1982**, *104*, 2797.
14. Pietro, W. J.; Francl, M. M.; Hehre, W. J.; Defrees, D. J.; Pople, J. A.; Binkley, J. S. *J. Am. Chem. Soc.* **1982**, *104*, 5039.
15. Gill, P. E.; Murray, W.; Wright, M. H. *Practical Optimization*; Academic Press, Inc.: New York, 1981.

Preparation and Characterization of Titanium Dioxide Embedded onto ZSM-5 Zeolite

A. Yu. Stakheev†, C. W. Lee, and P. J. Chong*

Advanced Materials Division, KRICT, P.O. Box 107, Yusung, Taejon 305-606, Korea
†N.D. Zelinsky Institute of Organic Chemistry, Leninskii Pr. 47, Moscow, Russia
Received October 19, 1997

Chemical vapor deposition of $TiCl_4$ followed by the hydrolysis thereof at elevated temperatures was employed for the formation of TiO_2 clusters inside ZSM-5 matrix. BET and XRD revealed that the zeolite structure remains intact. XPS, Raman, FTIR, and UV-VIS reflectance spectroscopy indicated that TiO_2 particles thus formed are extremely small and localized inside the zeolite matrix.

Introduction

Recently intensive research efforts have been directed toward the synthesis and characterization of "quantum-sized" semiconductor particles embedded inside zeolite framework.[1] Zeolites containing TiO_2 clusters may be of interest as a system for investigation into "quantum-size effect" (Q-size effect) and photoactive catalysts. Moreover, TiO_2-embedded zeolites may be useful for the preparation of shape-selective catalysts for the Fischer-Tropsch synthesis.[2]

Recently, two methods have been reported, whereby zeolite-hosted extra framework TiO_2 clusters are prepared.[3,4] These include ion exchange of Ti with ammonium titanyl oxalate aqueous solution, $(NH_4)_2TiO(C_2O_4)_2$, and chemical vapor deposition (CVD) of titanium by the treatment of zeolite with $TiCl_4$ vapors followed by the hydrolysis of the resulting material.

However, ZSM-5 zeolite containing TiO_2 clusters has not been prepared yet due to the difficulties in embedding of TiO_2 particles inside the narrow channel system of ZSM-5. The ion-exchange procedure does not allow the TiO_2 particles to be encapsulated inside the narrow pore zeolites (ZSM-5, mordenite, etc.), because TiO^{2+} are usually hydrated and too bulky to penetrate inside the zeolite pores. Treatment of the zeolite with $TiCl_4$ vapors appears to be more promising, but suffers from the damage of zeolite structure by HCl evolved due to the concurrent hydrolysis.

The main aims of this research are;

1) to develop the procedures for the encapsulation of ultra-fine nano-scale TiO_2 particles in ZSM-5 channels, which will not damage zeolite structure,

2) to study the effect of the TiO_2 inclusion on the zeolite structure, and

3) to characterize the resultant materials using relevant physico-chemical methods.

*To whom correspondence should be addressed.

Experimental

Sample preparation. ZSM-5 containing TiO_2 were prepared by chemical vapor deposition (CVD) of $TiCl_4$ onto HZSM-5 (Si/Al=15, PQ Co.). The order of preparative procedures are as follows:

1. Calcination
2. CVD of $TiCl_4$
3. Removal of excess $TiCl_4$
4. Hydrolysis of embedded $TiCl_4$

3-5 g of the zeolite powder was accurately weighed and loaded into a flow reactor with a diameter of 50 mm, which permits shallow bed spreads. It was calcined in O_2 flow overnight at 500 °C. Thereafter, dry helium was admitted with no further flow of oxygen. The experimental temperature was adjusted to 250-400 °C and CVD was performed for 3-4 hours. $TiCl_4$ vapor was diluted (1 : 10) with pure He so that the zeolite surfaces may not be damaged by the HCl evolved during the interaction of $TiCl_4$ with zeolite surface OH-groups. The overall flow rate of the mixed gas was about 300 mL/min. Treatment with $TiCl_4$ vapor was continued, until excess $TiCl_4$ was not observed in gas-wash bottle. Upon completion of the CVD step, the reactor was flushed for at least 2 hours at 500 °C to remove excess $TiCl_4$. Chemisorbed $TiCl_4$ was then hydrolyzed at 300-450 °C by a water vapor present in the flow of N_2. N_2 flow saturated with H_2O vapor was used after dilution (1 : 10) with pure N_2.

Sample characterization. The crystallinity of the samples was checked by X-ray diffraction (XRD) of the zeolite powder using a Rigaku D/MAX-3B diffractometer for which Cu-Kα radiation is employed. BET surface area was measured by physisorption of N_2 using a Micromeritics model, ASAP 2400. Raman spectra were measured by a